International Journal of Modern Physics C, Vol. 11, No. 5 (2000) 1013–1024

MOLECULAR-DYNAMICS SIMULATIONS OF NICKEL CLUSTERS

ŞAKIR ERKOÇ*
Department of Physics, Middle East Technical University
06531 Ankara, Turkey
E-mail: *erkoc@erkoc.physics.metu.edu.tr*

BILAL GÜNEŞ and PERVIN GÜNEŞ
Fizik Bölümü, Gazi Eğitim Fakültesi
Gazi Üniversitesi, 06500 Ankara, Turkey

Received 28 July 2000
Revised 29 July 2000

Structural stability and energetics of nickel clusters, Ni_N ($N = 3-459$), have been investigated by molecular-dynamics simulations. A size-dependent empirical model potential energy function has been used in the simulations. Stable structures of the microclusters with sizes $N = 3 - 55$ and clusters generated from fcc crystal structure with sizes $N = 79 - 459$ have been determined by molecular-dynamics simulations. It has been found that the five-fold symmetry appears on the surface of the spherical clusters. The average coordination number shows a size-dependent characteristic, on the other hand the average nearest-neighbor distance does not show a size-dependence.

Keywords: Nickel Clusters; Empirical Potentials; Molecular-Dynamics.

PACS Nos.: 36.40.−c, 36.40.Qv, 61.46.+w, 02.70.Ns

1. Introduction

Clusters play an important role in understanding the transition from microscopic structure to macroscopic structure of matter. At very small cluster sizes, the structures are molecular where at large cluster sizes, they are bulk like. It is the intermediate region in which the properties and structures change between these limits. The research field of clusters, particularly microclusters, has shown a rapid development in both experimental and theoretical investigations in the last decade.[1,2] The geometrical structure of clusters is undoubtedly important in understanding physical and chemical properties in processes such as catalysis,

*Corresponding author.

sintering, and cluster assembled interfaces.[3] Although there are considerable improvement in the experimental techniques, there are still difficulties in the production and/or investigation of isolated microclusters of some elements. Transition metal clusters have been investigated experimentally by the use of chemical probes[4] that determine the number and types of binding sites, but cannot determine directly the structure. Computer simulations provide help for a deeper understanding of the experimental observations in one hand, and they can also be applied for the systems which are practically difficult to make experiments on the other hand. Atomistic level computer simulations using empirical model potentials have been used successfully in investigating bulk, surface, and cluster properties of elements. In the literature, there are many empirical potential energy functions which are proposed and applied to various systems in the last decade.[5,6]

Nickel clusters are interesting and have potential importance in the physics and chemistry of transition metals.[7] Nickel clusters are of special interest because of their practical applications in ferromagnetism and their superparamagnetic behavior.[8,9]

There exist several experimental[8−12] and theoretical[13−32] studies of nickel clusters. Density functional theory (DFT) method was used to investigate the structural and electronic properties of nickel clusters upto 13 atoms[13] and for Ni_5 and Ni_6 clusters.[14] Empirical potential energy functions (EPEF) were used to study the structural properties of nickel clusters upto 40 atoms,[15] 55 atoms,[16] 4 atoms,[17] and 7 atoms.[18] Tight-binding molecular-dynamics (TB-MD) method was used to investigate the magnetic properties of nickel clusters of sizes from 5 to 60 atoms,[19] from 2 to 6 atoms,[20] from 5 to 16 atoms,[21] from 2 to 7 atoms,[22] and structural properties of nickel clusters upto 55 atoms,[23] and upto 10 atoms.[24] Embedded atom (EA) method was used to study the structural properties of nickel clusters of sizes from 13 to 147 atoms,[25] and melting properties of nickel clusters upto 19 atoms.[26,27] Effective medium (EM) method was used to study the structural properties of nickel clusters of sizes from 4 to 23 atoms[28] and from 24 to 55 atoms.[29] Friedel's model was used to study the structural and magnetic properties of nickel clusters of sizes from 5 to 26 atoms.[30] Another EPEF was used to investigate the structural properties of nickel clusters of sizes upto 23 atoms.[31] EA method was used to study the energetics of nickel clusters of sizes from 142 to over 5000 atoms.[32]

In this work, we have investigated the structural properties of isolated nickel clusters containing 3 to 459 atoms. Using a recently developed empirical potential energy function for nickel,[6] we performed Molecular-Dynamics (MD) simulations to predict the stable structures of nickel clusters.

2. The Potential Energy Function

In this work, we have used for the first time a size-dependent empirical potential energy function (SDEPEF) developed for a finite system and parameterized for nickel.[6] The total interaction energy (Φ) of an N particle system may be calculated

from the sum of pair interactions and scaled by a size dependent function $f(N)$,

$$\Phi = f(N) \sum_{i<j}^{N} U(r_{ij}) \,. \tag{1}$$

The pair potential energy function $U(r)$ is in the form,[17,18]

$$U(r) = A \left[\left(\frac{r_0}{r} \right)^{2n} e^{-2\alpha(r/r_0)^2} - \left(\frac{r_0}{r} \right)^{n} e^{-\alpha(r/r_0)^2} \right] . \tag{2}$$

The size dependent function $f(N)$ is in the form,[6]

$$f(N) = \sqrt{\beta_1 + \beta_2/N} \,. \tag{3}$$

The potential parameters used for nickel are: $A = 8.28$, $r_0 = 2.2$, $n = 2.89247$, $\alpha = 0.693147181$,[17,18] and $\beta_1 = 0.081$, $\beta_2 = 1.532$.[6] In these parameters, energy is in eV and distance is in Å.

Using this SDEPEF, we have performed molecular-dynamics simulations to obtain the stable structures of nickel clusters with the number of atoms from 3 to 459.

3. Results and Discussion

The nickel clusters having 3 to 459 atoms have been investigated by performing molecular-dynamics simulation at constant temperature to obtain the stable structure of each cluster. The motion equations of the particles are solved by considering the Nordsieck–Gear algorithm[33,34] within the seventh order predictor-corrector method.[35] The simulations are carried out by starting at 600 Kelvin, then the temperature was reduced to 1 Kelvin in four stages, namely 600, 300, 100, and 1 Kelvin. We have done this procedure to increace the probability of catching the stable configuration of potential energy surface of the simulated cluster. This type of temperature reduction with smaller steps is already known in the literature; the simulated annealing method[36] is well known in the optimization of many-particle systems via the Monte Carlo type simulations. The sudden reduction of temperature does not change much the energetics of the system studied, however a slight change in the geometry may take place, which does not affect the conclusions in this work. A similar method was applied before for silver[37] and gold[38] clusters. The time step has been taken as 1.0×10^{-15} seconds. In the simulations, we have taken the number of MD steps at most 50 000 for clusters with the number of atoms from 3 to 55. In the last 10 000 steps, the temperature rescaling is turned off and the system was relaxed to reach the thermal equilibrium. For clusters with the number of atoms $N > 55$, the number of MD steps were taken as 90 000, again in the last 10 000 steps, the system allowed to relax and reach the thermal equilibrium. This steps were enough to reach the equilibrium in total energy and to get the thermal equilibrium of the system studied. We performed this procedure for every temperature reduction in the simulations.

Like conventional molecules, most clusters, in general, have some well-defined geometry corresponding to the absolute minimum energy of their potential surfaces. There might be many local minima on the potential energy surface of a many-particle system and also there might be many isomers of a many-particle system. In the present study, we have generated the microclusters starting from three particles. Adding one atom at a time, we relaxed the system by the temperature reduction procedure to obtain the stable structure of the considered cluster. We applied this method for microclusters with sizes $N = 3 - 55$. The stable structures of nickel clusters with sizes $N = 3 - 55$ obtained by the MD simulations are shown in Figs. 1(a), 1(b), and 1(c). These structures represent the configuration of the system studied at the last MD step. We have also simulated spherical nickel clusters, which are generated from the fcc crystalline structure by taking the fifth, sixth and so on upto 17th neighbors to a central atom in the bulk. The cluster models generated in this form contain the number of atoms $N = 79$, 87, 135, 141, 177, 201, 225, 249, 321, 369, 381, 429, and 459. We applied the same simulation procedure for these spherical clusters. The three-dimensional structures of these clusters are presented in Fig. 1(d).

The binding energy, namely the average interaction energy per atom in the cluster, versus the cluster size, the number of atoms in the cluster, is plotted for the stable structures in Fig. 2. The average binding energy per atom decreases as the cluster size increases, it shows an exponential like decaying. From the energetics point of view, we may classify the studied nickel clusters into three groups (3–13; 13–55; 55–459). In the first group of clusters, the variation of average binding energy

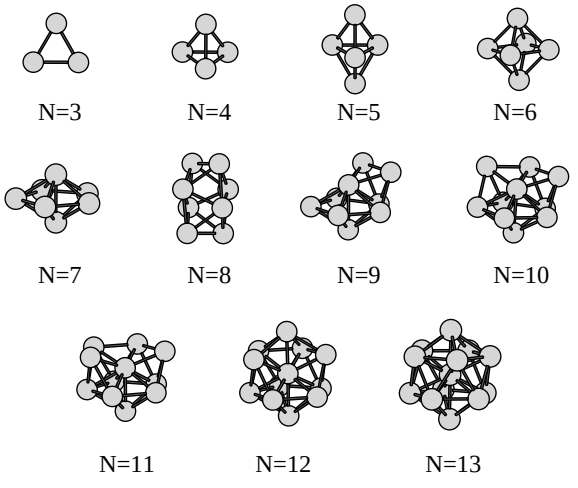

(a)

Fig. 1. The structures of energetically most stable nickel clusters, Ni_N. (a) for $N = 3 - 13$, (b) for $N = 13 - 40$, (c) for $N = 41 - 55$, and (d) for $N = 79 - 459$.

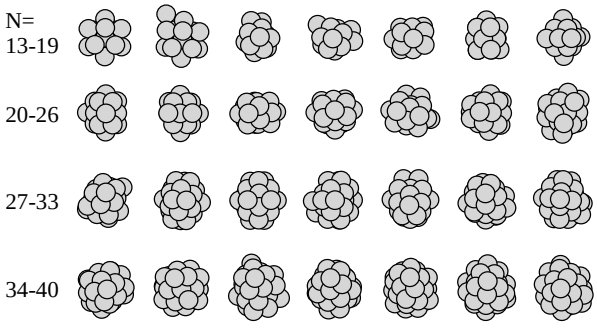

(b)

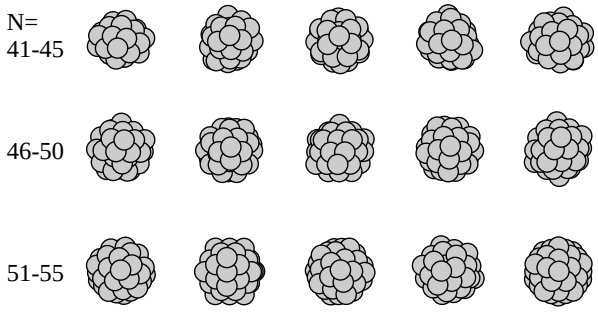

(c)

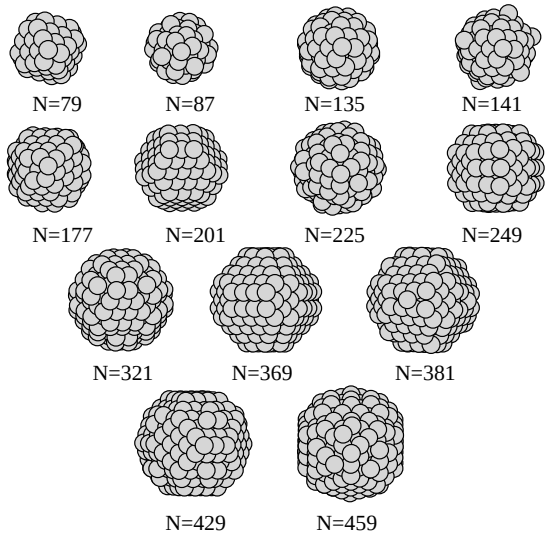

(d)

Fig. 1. (*Continued*)

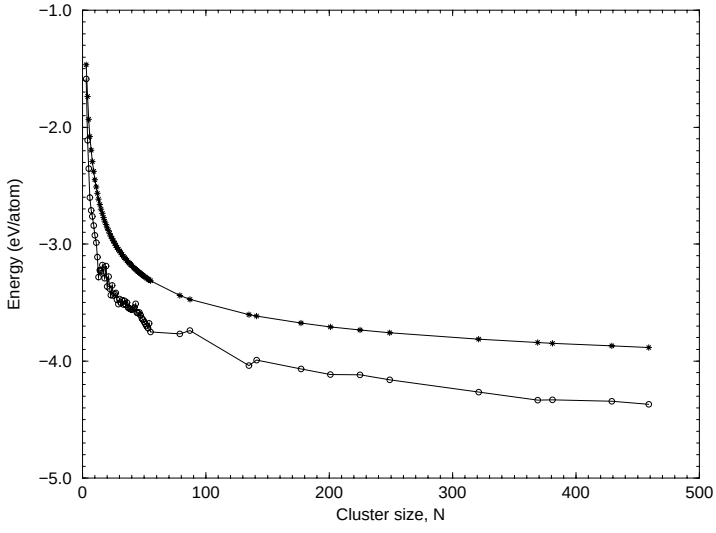

Fig. 2. The variation of average interaction energy, $E_b = E_N/N$, versus the cluster size (N), $N = 3 - 459$. Starred values are from Eq. (4).

with respect to the cluster size is fast. However, the variation of average binding energy with respect to the cluster size for the second group of clusters changes relatively slow. This trend appears in the third group of clusters even more slowly. The general decaying behavior in the average binding energy with respect to the cluster size is common almost for all metal clusters.[3] The size dependence of average binding energy per atom for metal clusters is predicted by the empirical relation,[2]

$$E_b(N) = \Phi + 2^{1/3}\left(\frac{1}{2}D_e - \Phi\right)N^{-1/3}\,, \tag{4}$$

here, Φ is the bulk cohesive energy of element forming the cluster, and D_e is the dimer binding energy. For nickel, $\Phi = -4.44$ eV/atom[39] and $D_e = -2.07$ eV.[40] Figure 2 contains also the binding energy variation with respect to the cluster size using Eq. (4). The functional dependence of both predicted [from Eq. (4)] and present calculation looks similar, but there is a small shift in the energy. One should not expect a perfect curve as obtained from Eq. (4) for finite size systems. Stability of clusters change from cluster to cluster; a size dependent fluctuation always exist in finite size systems, which shows the relative stability among the clusters. The variation of the average binding energy versus the cluster size for the number of atoms $3 - 55$ is shown in Fig. 3 to see the relative stability of microclusters clearly. On the other hand, for isolated clusters, the average binding energy per atom in the cluster $E_b = \Phi/N$ may also be expressed as a function of cluster size N,[3]

$$E_b = E_v + E_s N^{-1/3} + E_c N^{-2/3}\,, \tag{5}$$

where the coefficients E_v, E_s, and E_c correspond to the volume, surface, and curvature energies of the particles forming the cluster respectively. The variation of E_b

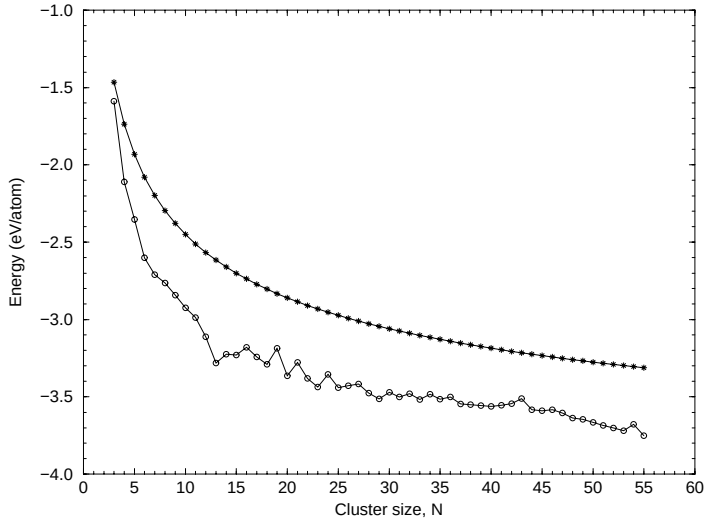

Fig. 3. The variation of average interaction energy, $E_b = E_N/N$, versus the cluster size (N), $N = 3 - 55$. Starred values are from Eq. (4).

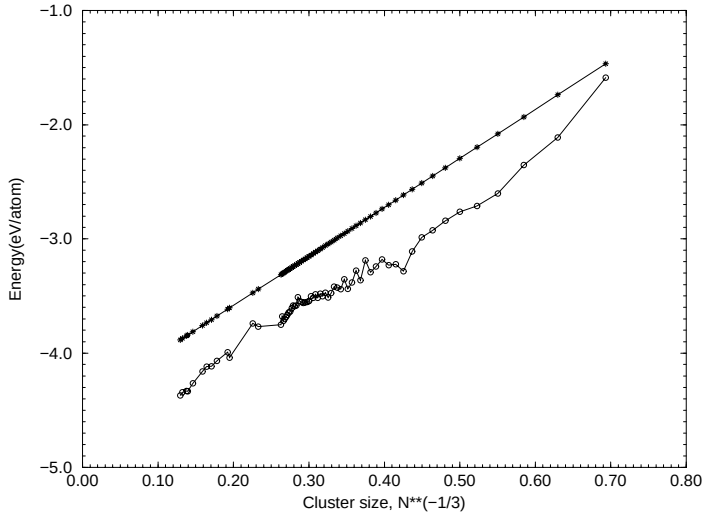

Fig. 4. The variation of average interaction energy, $E_b = E_N/N$, versus the cluster size ($N^{-1/3}$), $N = 3 - 459$. Starred values are from Eq. (4).

versus $N^{-1/3}$ is shown in Fig. 4. The linear fit of data to Eq. (5) gives $E_v = -4.842$ and $E_s = 4.237$, the quadratic fit gives $E_v = -4.738$, $E_s = 3.600$, and $E_c = 0.864$. The volume energy E_v corresponds to the bulk cohesive energy of the element considered is -4.44 eV/atom for nickel. The present calculation (quadratic fit) gives a result about 7% lower than the experimental value, which may be considered reasonable. Using the E_b values obtained from Eq. (4), linear fit gives

$E_v = -4.440$ and $E_s = 4.290$, the quadratic fit gives $E_v = -4.440$, $E_s = 4.290$, and $E_c = -0.879 \times 10^{-8}$. The volume energy obtained from the fit of data generated from Eq. (4) is equal to the experimental value, as expected. The plot of E_b versus $N^{-1/3}$ from Eq. (4) is also shown in Fig. 4.

The stable structures of the microclusters with sizes $n = 3 - 7$ have a regular symmetry. The corresponding point groups of these clusters are: $Ni_3(D_{3h})$, $Ni_4(T_d)$, $Ni_5(D_{3h})$, $Ni_6(O_h)$, and $Ni_7(D_{5h})$. On the other hand, the clusters with the sizes $N = 9-12$ seem to be formed by adding one by one to the seven-atom cluster. In these structures, the configuration of seven-atom cluster keeps its symmetry. However, the eight-atom cluster does not show this property, there is no pentagonal bipyramidal seed in the eight-atom cluster. The Ni_{13} has the symmetry I_h.

DFT calculation[13] gives the stable structure of Ni_3 as trigonal, Ni_4 as trigonal bipyramid and square, Ni_5 as trigonal bipyramid, Ni_6 as square bipyramid (or octahedron), Ni_8 as cube, and Ni_{13} as icosahedron. Another DFT calculation[14] gives Ni_5 as trigonal bipyramid, and Ni_6 as square bipyramid. An empirical potential energy function (EPEF) calculation[15] gives Ni_3 as trigonal, Ni_4 as trigonal pyramid, Ni_5 as trigonal bipyramid, Ni_6 as octahedron, Ni_7 as pentagonal bipyramid, Ni_8 as deformed central tetrahedron, and Ni_{13} as icosahedron. Another EPEF calculation[16] gives similar structures for $Ni_3 - Ni_{13}$ as found in the present work. Another EPEF calculation[16] gives similar structures for Ni_3 and Ni_4,[17] and for $Ni_3 - Ni_7$[18] as found in the present work. Tight-binding molecular-dynamics calculations[21,23] give similar structures for $Ni_3 - Ni_{13}$ as found in the present work. In an embedded atom method calculation,[25] the icosahedral structures of nickel clusters were studied. The effective medium calculations[28,29] give similar structures for $Ni_3 - Ni_{13}$ as found in the present work. Friedel's model calculation[30] predicted the structures of nickel clusters $Ni_5 - Ni_{14}$ as based on hexadron, and $Ni_{15} - Ni_{26}$ as based on cubic and hexagonal antiprism. Another EPEF calculation[31] gives similar structures for $Ni_3 - Ni_{23}$ as found in the present work. In another EA method calculation,[32] the various crystallite forms of large nickel clusters were investigated. In Ref. 32, it was found that the five-fold symmetry is favorable on spherical nickel clusters. Similar trend appears in the present calculations.

Experimental observations[12] show that Ni_3 is triangular, Ni_4 is not certain probably two-dimensional such as rhombic, Ni_5 is three-dimensional in trigonal bipyramid form, Ni_6 is octahedron, Ni_7 is in capped octahedron, Ni_8 is in bisdispheroid structure (D_{2d} dodecahedron), Ni_9 is in tricapped trigonal prism, Ni_{10} is in tricapped pentagonal bipyramid, Ni_{11} is not certain probably pentagonal, Ni_{12} is in icosahedron minus one atom, Ni_{13} is in icosahedron, Ni_{14} is in bicapped hexagonal antiprism, and finally Ni_{15} is in bicapped icosahedron form.

The average nearest neighbor distances (NND) vary around 2.2 Å at the last MD step for almost all the clusters considered. This value is equal to the experimental dimer distance of nickel-dimer, $r_e = 2.20$ Å.[40] The variation of NND versus the cluster size ($N = 3 - 459$) is shown in Fig. 5. It seems that NND does not show a dependence on the cluster size. On the other hand, the average coordination number

(CN) that is the average number of nearest neighbors, shows a dependence on the cluster size. The variation of CN versus the cluster size ($N = 3 - 459$) is shown in Fig. 5. The variation of CN versus the cluster size ($N = 3 - 55$) is shown in Fig. 6 to see the details clearly. The spherical clusters keep their spherical form after the relaxation, but atoms on the surface region reconstructed slightly with

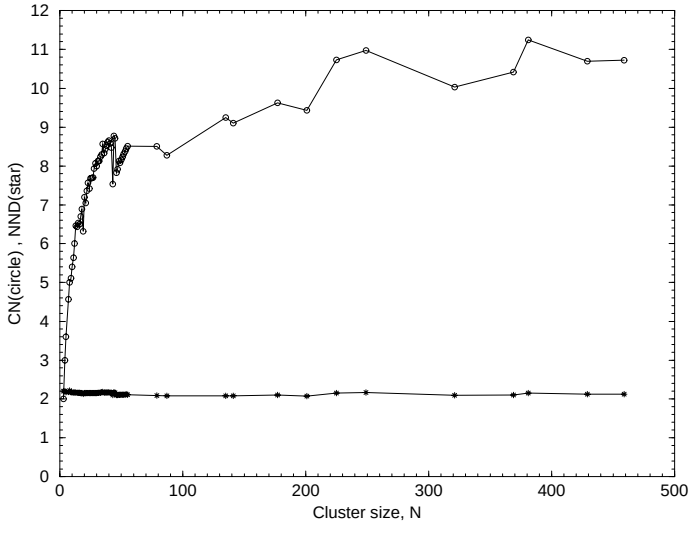

Fig. 5. The variation of average coordination number (CN) and the average nearest neighbor distance (NND) versus the cluster size (N), $N = 3 - 459$.

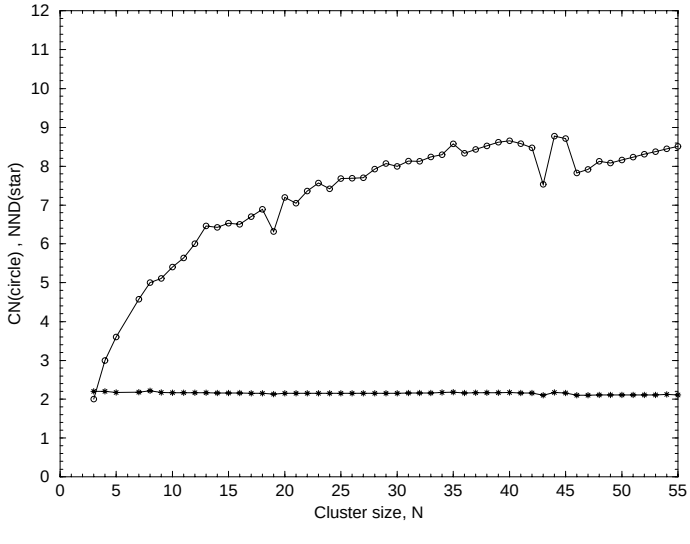

Fig. 6. The variation of average coordination number (CN) and the average nearest neighbor distance (NND) versus the cluster size (N), $N = 3 - 55$.

respect to the original positions. Five-fold symmetry appears on the surface region of relaxed spherical clusters; especially this feature appears on the clusters with sizes $N = 3 - 55$. This situation is clearly seen in Fig. 1. The icosahedral structure dominates at small cluster sizes and the *fcc* structure becomes more prominent at larger sizes. The structural change occurs because of competition between surface and bulk energy components. The icosahedral structure minimizes surface energy whereas the *fcc* structure minimizes bulk energy.

The relative stabilities of clusters can also be analyzed by considering the first and second difference energies, namely $\Delta E^{(1)} = E_N - E_{N-1}$ and $\Delta E^{(2)} = E_{N+1} - 2E_N + E_{N-1}$ respectively. In the limit of very large clusters, $\Delta E^{(1)}$ will approach to cohesive energy of the corresponding bulk solid. $\Delta E^{(1)}$ is a measure of how different the clusters are from their bulk limit in terms of stability. $\Delta E^{(2)}$ is the difference of energy of two fragmentation paths $X_{N+1} \to X_N + X$ and $X_N \to X_{N-1} + X$. If $\Delta E^{(2)} > 0$, it means that the dissociation of X_{N+1} into X_N leaving one atom free is more favorable than the dissociation of X_N into X_{N-1}, so, $\Delta E^{(2)}$ is nothing but a measure of stability of clusters. The variation of $\Delta E^{(1)}$ and $\Delta E^{(2)}$ with respect to the cluster size are shown in Figs. 7 and 8 respectively. From Fig. 3, one may say that the clusters with the number of atoms $N = 13$, 18, 20, 23, 25, 29, 37, 44, 53, and 55 seem to be relatively more stable; from Fig. 7, the clusters with the number of atoms $N = 4$, 13, 17, 20, 22, 25, 28, 31, 33, 35, 37, 44, and 55 seem to be relatively more stable; from the Fig. 8, the clusters with the number of atoms $N = 4$, 6, 13, 18, 20, 23, 25, 29, 33, 44, and 53 seem to be more stable. We may conclude that the common numbers in these three sets of numbers might be the magic numbers for the studied nickel clusters in the present work for the range of

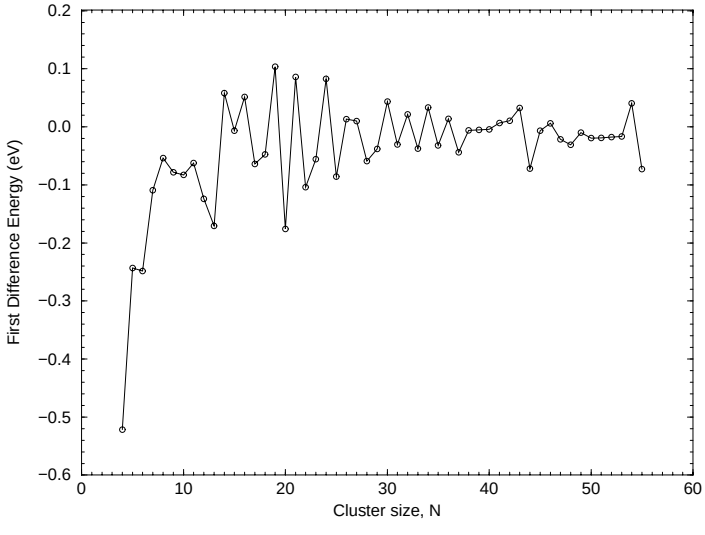

Fig. 7. The variation of first difference in the total energy, $\Delta E_N^{(1)}$, versus the cluster size (N), $N = 3 - 55$.

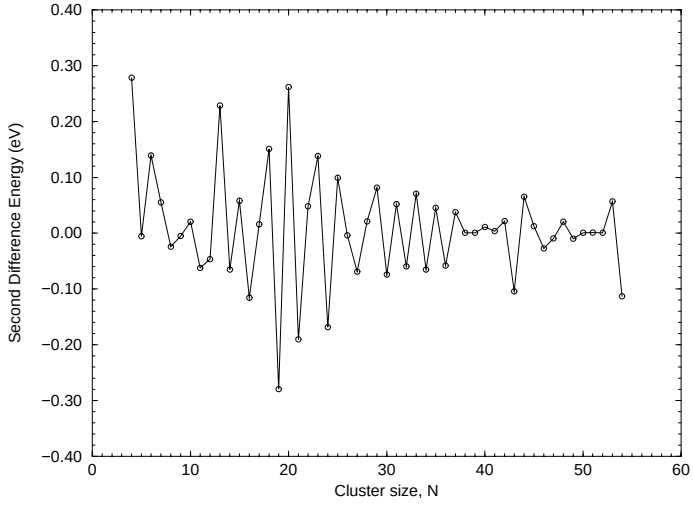

Fig. 8. The variation of second difference in the total energy, $\Delta E_N^{(2)}$, versus the cluster size (N), $N = 3 - 55$.

cluster size $3 \leq N \leq 55$. The common numbers are $N = 13$, 20, 25, and 44. We may call these numbers as the primary magic numbers for nickel microclusters. The numbers appearing in at least two groups, $N = 4$, 18, 23, 29, 33, 37, and 53 might be the secondary magic numbers for nickel microclusters.

We have investigated the structural stability and energetics of isolated nickel clusters containing 3 to 459 atoms. As a conclusion, we may say that nickel microclusters prefer to form three-dimensional compact structures. On the other hand, five-fold symmetry appears on the surface region of spherical clusters. The average coordination number shows a size-dependent behavior, however, the average nearest neighbor distance seems to be size-independent.

Acknowledgments

One of the authors (ŞE) would like to thank TUBITAK (Scientific and Technical Research Council of Turkey) for partial support through the project TUBITAK–AY/194.

References

1. S. Sugano, Y. Nishina, and S. Ohnishi (eds.), *Microclusters* (Springer-Verlag, 1987).
2. H. Haberland (ed.), *Clusters of Atoms and Molecules* (Springer-Verlag, 1994).
3. G. Scoles (ed.), *The Chemical Physics of Atomic and Molecular Clusters* (North Holland, 1990).
4. E. K. Parks and S. J. Riley, *Z. Phys. D* **33**, 59 (1995).
5. Ş. Erkoç, *Phys. Reports* **278**, 79 (1997).
6. Ş. Erkoç, in *Ann. Rev. Comp. Phys.* Vol. IX, ed. D. Stauffer (World Scientific, 2001).
7. V. Bonacic–Koutecky, P. Fantucci, and J. Koutecky, *Chem. Rev.* **91**, 1035 (1991).

8. I. M. L. Billas, J. A. Becker, A. Chatelain, and W. A. de Heer, *Science* **265**, 1682 (1994).
9. S. E. Aspel, J. W. Emmert, J. Deng, and L. A. Bloomfield, *Phys. Rev. Lett.* **76**, 1441 (1996).
10. M. R. Zakin, D. M. Cox, R. O. Brickman, and A. Kaldor, *J. Phys. Chem.* **93**, 6823 (1989).
11. M. Pellavin, B. Baguenard, J. L. Viella, J. Lerme, M. Broyer, J. Miller, and A. Perez, *Chem. Phys. Lett.* **217**, 349 (1994).
12. E. K. Parks, L. Zhu, J. Ho, and S. J. Riley, *J. Chem. Phys.* **100**, 7206 (1994).
13. F. A. Reuse and S. N. Khanna, *Chem. Phys. Lett.* **234**, 77 (1995).
14. M. C. Michelini, R. P. Diez, and A. H. Jubert, *J. Mol. Struc. (Theochem)* **490**, 181 (1999).
15. W. J. Hu, L. M. Mei, and H. Li, *Solid State Commun.* **100**, 129 (1996).
16. A. P. Amerillas and I. Garzon, *Phys. Rev. B* **54**, 10362 (1996).
17. Ş. Erkoç, *Phys. Stat. Sol. (b)* **152**, 447 (1989).
18. Ş. Erkoç, *Phys. Stat. Sol. (b)* **161**, 211 (1990).
19. F. A. Granja, S. Bouarab, M. J. Lopez, A. Vega, J. M. M. Carrizales, M. P. Inigues, and J. A. Alonso, *Phys. Rev. B* **57**, 12469 (1998).
20. A. N. Andriotis and M. Menon, *Phys. Rev. B* **57**, 10069 (1998).
21. S. Bouarab, A. Vega, M. J. Lopez, M. P. Inigues, and J. A. Alonso, *Phys. Rev. B* **55**, 13279 (1997).
22. A. N. Andriotis, N. Lathiotakis, and M. Menon, *Chem. Phys. Lett.* **260**, 15 (1996).
23. N. N. Lathiotakis, A. N. Andriotis, M. Menon, and J. Connolly, *J. Chem. Phys.* **104**, 992 (1996).
24. M. Menon, J. Connolly, N. Lathiotakis, and A. Andriotis, *Phys. Rev. B* **50**, 8903 (1994).
25. J. M. M. Carrizales, M. P. Iniguez, J. A. Alonso, and M. J. Lopez, *Phys. Rev. B* **54**, 5961 (1996).
26. I. L. Garzon and J. Jelinek, in *Physics and Chemistry of Finite Systems: From Clusters to Crystals*, eds. P. Jena, S. N. Khanna, and B. K. Rao (Kluver, 1992), p. 405.
27. Z. Guvenc, J. Jelinek, and A. Voter, in *Physics and Chemistry of Finite Systems: From Clusters to Crystals*, eds. P. Jena, S. N. Khanna, and B. K. Rao (Kluver, 1992), p. 411.
28. M. S. Stave and A. E. DePristo, *J. Chem. Phys.* **97**, 3386 (1992).
29. T. L. Wetzel and A. E. DePristo, *J. Chem. Phys.* **105**, 572 (1996).
30. F. A. Granja, J. M. M. Carrizales, and J. L. M. Lopez, *Solid State Commun.* **105**, 25 (1998).
31. S. K. Nayak, S. N. Khanna, B. K. Rao, and P. Jena, *J. Phys. Chem. A* **101**, 1072 (1997).
32. C. L. Cleveland and U. Landman, *J. Chem. Phys.* **94**, 7376 (1991).
33. A. Nordsieck, *Math. Comp.* **16**, 22 (1962).
34. C. W. Gear, *Numerical Initial Value Problems in Ordinary Differential Equations* (Prentice-Hall, 1971).
35. D. J. Evans and G. P. Morriss, *Computer Phys. Rep.* **1**, 299 (1984).
36. S. Kirkpatrick, C. D. Gelatt, and M. P. Vecchi, *Science* **220**, 671 (1983).
37. Ş. Erkoç and T. Yilmaz, *Physica E* **5**, 1 (1999).
38. Ş. Erkoç, *Physica E* **8**, 210 (2000).
39. C. Kittel, *Introduction to Solid State Physics*, 4th edition (Wiley, 1971).
40. M. D. Morse, *Chem. Rev.* **86**, 1049 (1986).